

Mineral Processing and Extractive Metallurgy Review

An International Journal

ISSN: 0882-7508 (Print) 1547-7401 (Online) Journal homepage: <https://www.tandfonline.com/loi/gmpr20>


A Novel Procedure for Performance Assessment of Paste Thickeners

Farhad Moosakazemi, Mohammad Hayati, Mohammad Reza Tavakoli
Mohammadi, Elmira Tajvidi Asr & Seyed Mohammad Javad Koleini

To cite this article: Farhad Moosakazemi, Mohammad Hayati, Mohammad Reza Tavakoli Mohammadi, Elmira Tajvidi Asr & Seyed Mohammad Javad Koleini (2019): A Novel Procedure for Performance Assessment of Paste Thickeners, Mineral Processing and Extractive Metallurgy Review, DOI: [10.1080/08827508.2019.1666127](https://doi.org/10.1080/08827508.2019.1666127)

To link to this article: <https://doi.org/10.1080/08827508.2019.1666127>

 View supplementary material 

 Published online: 25 Sep 2019.

 Submit your article to this journal 

 View related articles 

 View Crossmark data 



A Novel Procedure for Performance Assessment of Paste Thickeners

Farhad Moosakazemi^a, Mohammad Hayati^b, Mohammad Reza Tavakoli Mohammadi^a, Elmira Tajvidi Asr^c, and Seyed Mohammad Javad Koleini^d

^aBeneficiation and Hydrometallurgy Research Group, Mineral Processing Research Center, Academic Center for Education, Culture and Research (ACECR) on TMU, Tehran, Iran; ^bMining Engineering Group, Faculty of Engineering, Lorestan University, Khorramabad, Iran; ^cSchool of Mining, Petroleum & Geophysics Engineering, Shahrood University of Technology, Semnan, Iran; ^dMineral Processing Department, Tarbiat Modares University, Tehran, Iran

ABSTRACT

High stability and low settling rate of phosphate fines in water suspensions encountered the dry area-located mines with serious environmental and technical challenges. The best suggestion for these mines is paste thickener installation for dewatering. In this research, the novel procedure has been proposed for evaluating the potential of paste thickeners in dewatering mining tailings. The case study is Esfordi phosphate complex (Iran). Initially, the selection criteria of a proper flocculant (environmental effects, price, particle settling rate, turbidity of overflow water, and underflow water content) were evaluated for current consuming flocculant (A-27) and 12 other ionic and nonionic flocculants. Then, flocculation performance was ranked based on the type and concentration, applying multiple criteria decision-making (MCDM) techniques of ORESTE, MAPPAC, and ELECTRE. Subsequently, the pilot-scale tests were performed for the selected flocculants and the operational conditions were evaluated for the maximum underflow solid content of 70 wt.%. The results of the present research showed that installation and application of this type of thickener could be effective for the case study.

KEYWORDS

Paste thickener; phosphate tailings; flocculant; multiple criteria decision-making techniques

1. Introduction

The problems associated with phosphatic clay management have encouraged the researchers to find economical and practical methods for dewatering and consolidating. These methods were documented in the literature (Boshoff, Morkel and Naude 2018; El-Shall and Zhang 2004; Garmsiri and Nosrati 2019; Gnandi et al. 2005; Kong and Orazem 2014; Ozacar and Ayhan Sengil 2003; Scheiner and Smelley 1985).

Although, storing phosphate tailings in clay ponds has been the most common method for disposal but now a more effective approach is followed by the industries to cover issues including a huge amount of water loss, occupying large pieces of land, and the possibility of environmental disasters (Besra, Sengupta and Roy 1998; Rulyov, Dontsova and Korolyov 2005; Tao, Parekh and Honaker 2008).

According to a research carried out for dewatering disposal in Esfordi phosphate complex (Iran), the lowest cost method for tailings disposal considering environmental conditions of the area is reported to be tailings dewatering by paste thickeners and transferring the slurry by capable pumps to the dam. Consequently, replacing conventional thickeners with paste thickeners (also known as deep cone thickeners) was chosen as an effective practical approach. Considering the importance of the subject, this research was conducted in two parts to investigate the feasibility of using paste thickener for the complex.

The first step to achieve optimum dewatering results is choosing the type and concentration of the flocculant in batch scale experiments. These flocking agents depending on the type and consuming dosage significantly influence particle settling rate, turbidity of overflow water, and underflow water content. Although, they can impose both operational cost and environmental effects on the mineral processing industry. In this research, the mentioned criteria were evaluated for the current flocculant of the complex (A-27) and 12 other ionic and nonionic flocculants. Obviously, an effective flocculant was identified with low consuming dosage, high particle settling rate, low turbidity of overflow water, and low underflow water content. Therefore, given the multiplicity of conflicting criteria and necessity of choosing the effective type and concentration of flocculants, multiple criteria decision-making (MCDM) techniques were applied in this study. MCDM techniques used in the mining research were mainly focused on its environmental effects and less on mineral processing. A summary of this research is given in Table 1.

In this research, to determine the type and concentration of the flocculant with respect to five criteria, MCDM techniques of ORESTE, MAPPAC, and ELECTRE (supplementary file) were applied for the first time in mineral processing field. The validation of ranking results was carried out using the three techniques. Precise selection of type and concentration of flocculant improves the results of subsequent pilot settling

CONTACT Mohammad Reza Tavakoli Mohammadi  r.tavakoli@acecr.ac.ir  Beneficiation and Hydrometallurgy Research Group, Mineral Processing Research Center, Academic Center for Education, Culture and Research (ACECR) on TMU, Tehran, Iran

Color versions of one or more of the figures in the article can be found online at www.tandfonline.com/gmpr.


 Supplemental data for the article can be accessed [here](#).

Table 1. Summary of the environment and mineral processing research using MCDM techniques.

Field	Subject	Evaluation technique	Reference
Environment	Environmental evaluation for sustainable development of coal mining in Qijiang, Western China	AHP	Si et al. (2010)
	Proposing a fuzzy decision support system for design of post-mining regions restoration and application of that system for decision making concerning the direction of revitalization in an open-cast mining institution in Poland	Fuzzy	Bielecka and KrolKorcak (2010)
	Proposing an integrated model in the framework of strengths, weaknesses, opportunities, and threats (SWOT) for ranking the strategies of Iranian mining sector	TOPSIS and ANP	Azimi et al. (2011)
	Development of a new model for geo-environmental impact assessment of mining, using a fuzzy synthetic ranking method	Fuzzy and AHP	Huang, Li and Wang (2012)
	Evaluation and ranking the sustainable water management in operating stage for six coal mines located in Australia	AHP, Fuzzy TOPSIS	Zhang et al. (2013)
	Identification the impacts of waste dumps generated from underground coal mining on the environment, describing the application of waste characterization for predicting environmental impacts over the site and also determining the preferred post-mining land use for the dumps	AHP	Adibee, Osanloo and Rahmanpour (2013)
	Geological environmental impact assessment of coal mining subsidence area in China	Fuzzy	Xu, Zhao and Li (2014)
	Negative environmental impacts assessment of exploitation from gravel and sand deposits in Poland in order to protect regions in the European Union	AHP and Leopold Matrix	Sobczyk, Kowalska and Sobczyk (2014)
	Risk assessment and ranking of polluting metals in copper mine sediments	FDAHP and TOPSIS	Hayaty et al. (2014)
	Human health and safety risks management in underground coal mines for controlling measurements and support decision making	Fuzzy TOPSIS	Mahdevari, Shahriar and Esfahanipour (2014)
Mineral processing	Development of a sustainable development framework for mining industries to assess the relative importance of different green supply chain management criteria	AHP	Shen, Muduli and Barve (2015)
	Selection of mineral processing plant location at the Sangan iron ore mine (phase 1) based on distance from the mine, access to heavy machinery transport, the amount of excavation required for grading, bed mixture capacity, belt conveyor length, distance from the tailings dam, distance from the waste dumps and surface water diversion requirements	AHP	Safari et al. (2010)
	Selection of the best primary crusher for Golegozar Iron Mine in Iran based on criteria such as capacity, feed size, product size, rock compressive strength, abrasion index and mobility of crusher	AHP	Rahimdel and Ataei (2014)
	Selection of collector and its dose rate in the flotation of lead-zinc sulfide ore	TOPSIS	Kostovic and Gligoric (2015)
	Selection of alunite processing method based on 14 technical, economic and environmental analyzing criteria	DAHP & Fuzzy TOPSIS	Alizadeh, Salari Rad and Bazzazi (2016)

experiments and enhances the capability of paste thickener for this complex. The novel procedure proposed in this research can be considered as a basis for evaluating the potential of paste thickeners in dewatering of mining tailings.

2. Materials and methods

2.1. Ore sample

The ore sample was received from Esfordi phosphate complex taken from the entrance launder of pulp to the thickener. The ore was filtered and dried. Characterization of the sample by X-ray powder diffraction (XRD) revealed that hematite, quartz, and fluorapatite were major phases, while, chlorite, talc, hornblendes, calcite, orthoclase, and dolomite were minor phases. Particle size distribution was measured by a particle size analyzer (Fritsch, "ANALYSETT 22"). Accordingly, arithmetic and geometric mean diameters of the particles were calculated as 10.7 μm and 6.5 μm , respectively, indicating the obstacle in settling. The natural settling rate of ore was obtained as 0.0066 cm/min.

2.2. Flocculants

Flocculation occurs by polymer bridging, charge compensation or neutralization, polymer surface complex formation and depletion, and/or by a combination of these mechanisms (Mpofu, Addai-Mensah and Ralston 2004; Mpofu, Mensah and Ralston 2003; Onen, Beyazyuz and Yel 2017). This

process causes an increase in the settling rate, the improvement of overflow clarity and the increase in the thickener capacity by decreasing particle residence time. Polymers are widely used flocculants that can be synthesized in various molecular masses and ionic forms (Gregory and Barany 2011; Kim and Palamino 2009). Consumed flocculants in this research were cationic (DHMW, EHMW, GHMW, and BHMW), anionic (A-26, A-27, A-100, A-110, A-130, A-150, X0, and X1), and nonionic (N-100). A-27 (Isfahan Copolymer Co., Iran) is the current consuming flocculant in the Esfordi phosphate complex.

2.3. Settling experiments

Settling experiments were conducted in a graduated cylinder with a capacity of 1000 ml and 35 cm of height. A 5% w/v slurry was provided for each settling experiment similar to the current solid percentage of the industrial thickener set. The normal pH of the slurry was measured as 7.9. Then, flocculants with the concentrations of 2, 4, 5, and 7 g/t were added and were mixed well by moving a mixer up and down equipped with a net-like circular plate at a slow rate. To calculate the settling rate, bed height changes were recorded as a function of time. After conducting settling experiment, overflow water was completely rejected and underflow was weighed, and then was subjected to a vacuum filter for a specified time. Water content was calculated based on the ratio of water weight of underflow to the whole weight of

underflow. A WTW 655 IR turbidity meter was exploited to measure the turbidity of overflow water. The results of batch scale settling experiments for settling rate, turbidity, and water content are presented in Figures S-1, S-2, and S-3, respectively, in the supplementary file.

Settling experiments were carried out using a pilot-scale paste thickener, schematic diagram and dimensions of which is shown in Figure 1a. This thickener was constructed by colorless Plexiglas to monitor the exact settling behavior, characterizing different zones including clear water, hindered settling, and compression and also determining pulp solid content profile in the zones. Furthermore, it contributes in evaluating the paste flow behavior from underflow and the effects of operational variables such as bed height and residence time on underflow solid content. Some sampling faucets with determined distances were embedded on the thickener wall. This thickener is fed with a height adjustable feed well designated for mixing the pulp with flocculant prior to introducing the settling part (Figure 1b). The height adjustability of the feed well avoids short circuiting and interference of overflow clear water with introducing pulp.

Pilot settling experiments were performed in both continuous and non-continuous state. In the non-continuous state, pulp and flocculant solution were introduced to the

thickener at 3 m height through the feed well, where the thickener was filled with water. Then, bed line height was measured at different times, until it reached up to 3 m height from the bottom of settling column. In the continuous state, the thickener was fed using the non-continuous state to reach the desired level. Then, feeding process continued for 5 h to achieve steady state, in other words, to have the same rate of solid content in both feeding and underflow.

2.4. Slump test

The slump test is used extensively by the engineers to estimate the yield stress and viscosity of paste (Tao, Parekh and Honaker 2008). This test was carried out using a PVC cylinder with height to diameter ratio of 1:1 under different conditions. First, paste with solid contents of 65%, 70%, and 75% was prepared using a mixture containing 5 g/t A-130 flocculant, solid sample and water. The cylinder was placed on a smooth surface and prepared pastes with different solid contents were added until it was filled. Then, the cylinder was taken upward slowly and the paste was let to flow.

As shown in Figure 2, the difference between the initial and final heights (center point of collapsed paste) was measured as a slump.

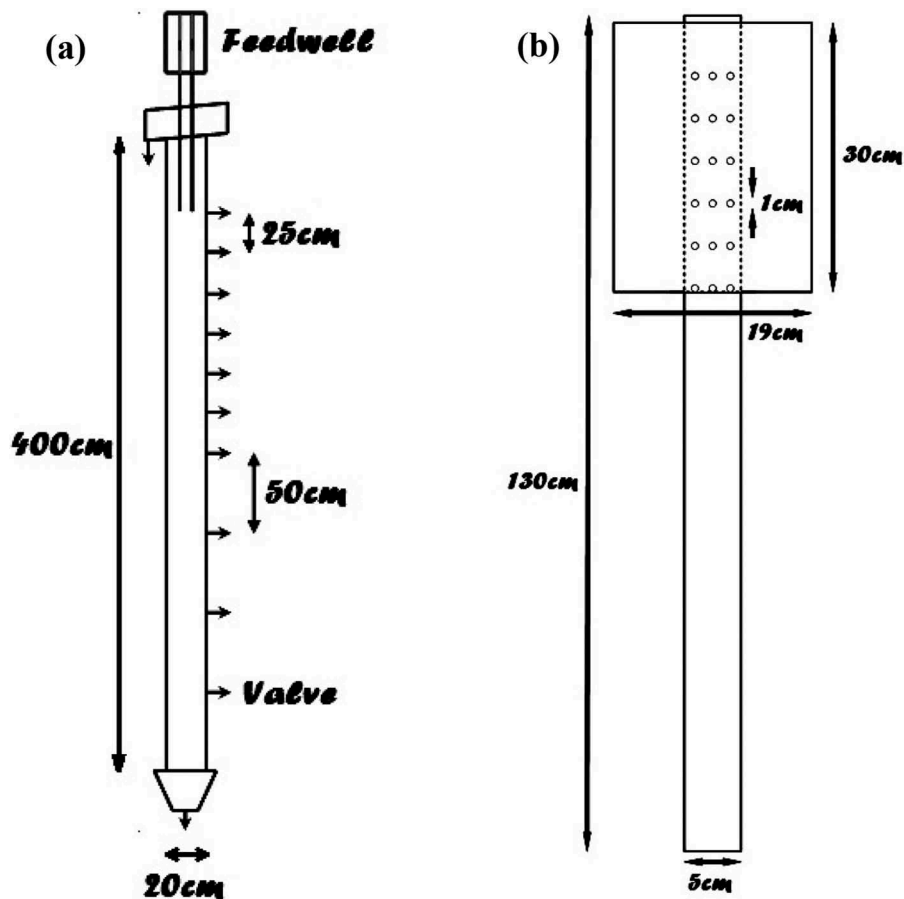


Figure 1. Schematic diagram and dimensions of the designed paste thickener (a) and feed well (b).

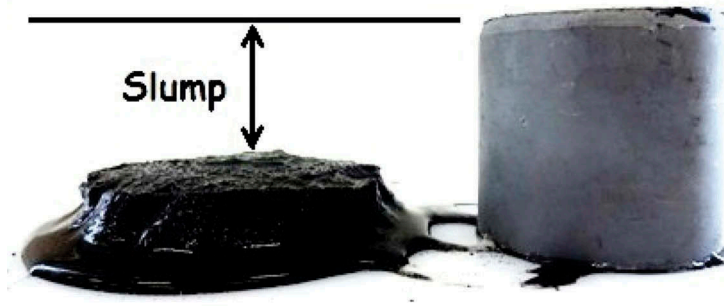


Figure 2. The measurement method of slump.

By measuring the density of produced pastes, yield stress (τ) could be calculated as in Eq. (1) (Tao, Parekh and Honaker 2008):

$$\tau = \left(O.S - O.S\sqrt{\frac{S}{H}} \right) \times \rho \times g \times h \quad (1)$$

where S is the difference between initial and final height (m), H is the initial height (m), g is gravitational acceleration (m/s^2), and ρ is paste density (kg/m^3).

3. Results and discussion

3.1. Selection of flocculant type and concentration

In this research, the current flocculant used in the plant (A-27) and 12 other ionic and nonionic flocculants were evaluated with respect to the above criteria. Then, flocculants were ranked according to the type and concentration using MCDM techniques of ORESTE, MAPPAC, and ELECTRE.

Regarding the calculations in MCDM techniques, the formation of decision matrix (R) is the first step. In this matrix, the element assigned to alternative i and criterion j is represented by r_{ij} so, this element indicates the characteristic of alternative i in the viewpoint of criteria j. 13 flocculants in 4 concentration levels were considered as the alternatives in the study defined as A1 to A52. Environmental effects of flocculants based on the consumption dosage (g/t), flocculant price (cent), particle settling rate (cm/min), turbidity of overflow water (NTU), and underflow water content (%) were evaluated as criteria defined as X1 to X5, respectively. Among all criteria, solely a decrease in the settling rate had a positive effect. The concentrations of flocculants were chosen as the value representing environmental effect for each alternative. Decision matrix was formed (Eq. (S-29)) with respect to alternative values for each criterion, as presented in the supplementary file. Due to the large volume of calculations and the large number of tables, only a few of them are presented in the following.

In the following, relative importance of criteria was determined according to experts' experience. For this purpose, 10 experts' opinions were collected using the ranking method where terms such as the least importance, less importance, mean importance, high importance, and the highest importance were assigned to 1, 2, 3, 4, and 5, respectively. The

average of experts' opinions was determined for the final weight, and then was normalized. In fact, the final weight is the ratio of the average of experts' opinion for each criterion to sum of experts' opinion averages for five criteria. Accordingly, the weights of 0.12, 0.26, 0.37, 0.09, and 0.16 were assigned to criteria of X1, X2, X3, X4, and X5, respectively.

3.1.1. Calculation stages in ORESTE technique

3.1.1.1. Primary ranking of alternatives. First, two preference structures were proposed for a set of criteria and alternatives in the decision matrix. The weights determined by the experts were applied to create the preference structure for criteria, and the second preference structure on the alternatives was similarly set based on each criterion. Then, Besson's average ranking method was applied to the initial ranking of criteria and alternatives set (Eq. (2)).

$$P = \begin{array}{c|ccccc} & X3 & X2 & X5 & X1 & X4 \\ \hline A1 & 52 & 12.5 & 17 & 7 & 51 \\ A2 & 44 & 1 & 1 & 7 & 30 \\ A3 & 45 & 3.5 & 36.5 & 7 & 37 \\ \dots & \dots & \dots & \dots & \dots & \dots \\ A50 & 15 & 38.5 & 39 & 46 & 15 \\ A51 & 16.5 & 48 & 48 & 46 & 3 \\ A52 & 11 & 46.5 & 50 & 46 & 4 \end{array} \quad (2)$$

3.1.1.2. Calculation of alternatives distances. In this study, direct linear estimation method was used to estimate distances in which the corresponding matrix is presented as shown in Eq. (3).

$$D = \begin{array}{c|ccccc} & X3 & X2 & X5 & X1 & X4 \\ \hline A1 & 41.273 & 9.935 & 13.518 & 5.882 & 40.491 \\ A2 & 34.923 & 1.651 & 2.410 & 5.882 & 23.848 \\ A3 & 35.717 & 2.941 & 28.975 & 5.882 & 29.391 \\ \dots & \dots & \dots & \dots & \dots & \dots \\ A50 & 11.907 & 30.559 & 30.959 & 36.518 & 12.051 \\ A51 & 13.097 & 38.099 & 38.101 & 36.518 & 4.236 \\ A52 & 8.733 & 36.908 & 39.688 & 36.518 & 4.555 \end{array} \quad (3)$$

3.1.1.3. Global ranking of distances. In this step, first, the prior results were ranked by Besson's average ranking method to achieve global ranks ($R(m_k)$). Then, $R(m)$ with value equal to the sum of $R(m_k)$ was calculated for each alternative (Eq. (4)).

Table 2. Alternatives ranking by ORESTE technique.

Rank	Alt.	Rank	Alt.	Rank	Alt.	Rank	Alt.
1	A28	14	A6	26	A18	38	A31
2	A35	15	A30	27	A32	39	A50
3	A15	16	A45	28	A49	40	A46
4	A41	17	A5	29	A19	41	A43
5	A2	18	A25	30	A37	42	A8
6	A9	19	A20		A4	43	A52
7	A7	20	A39	31	A1	44	A51
8	A22	21	A24	32	A29	45	A14
9	A12	22	A3	33	A42	46	A27
10	A48	23	A26	34	A23	47	A21
11	A13	24	A17	35	A33	48	A40
12	A11	25	A16	36	A36	49	A34
13	A10	26	A44	37	A38	50	A47

Table 3. Alternatives ranking in MAPPAC technique.

Rank	Alt.	Rank	Alt.	Rank	Alt.	Rank	Alt.
1	A28	11	A20	23	A42	33	A46
2	A15		A25	24	A4	34	A33
	A35	12	A39	25	A38	35	A52
	A41	13	A5		A44	36	A43
3	A2	14	A6	26	A45	37	A27
4	A9	15	A30	27	A18		A51
5	A7	16	A49	28	A19	38	A8
	A22	17	A17	29	A32	39	A1
6	A48	18	A37	30	A23	40	A14
7	A13	19	A3		A31		A34
8	A12	20	A26	31	A29		A40
9	A10	21	A24		A50	41	A21
10	A11	22	A16	32	A36	42	A47

$$R = \begin{matrix} & X3 & X2 & X5 & X1 & X4 & R(m) \\ A1 & 258 & 61.5 & 79 & 33 & 257 & 688.5 \\ A2 & 214 & 2.5 & 5.5 & 33 & 146 & 401 \\ A3 & 217 & 8.5 & 183.5 & 33 & 187 & 629 \\ \dots & \dots & \dots & \dots & \dots & \dots & \dots \\ A50 & 70 & 191.5 & 194 & 228 & 72 & 755.5 \\ A51 & 77.5 & 242 & 243 & 228 & 17.5 & 808 \\ A52 & 54 & 236.5 & 249 & 228 & 19 & 786.5 \end{matrix} \quad (4)$$

Finally, ranking of alternatives was performed according to R(m) results as shown in Table 2. In ORESTE technique, a better ranking is given to the alternative with smaller R(m).

3.1.2. Calculation steps in MAPPAC technique

3.1.2.1. Determination of normalized decision matrix, C. In the first step of ranking, using these technique ideal values of 5, 2.86, 13.34, 321.9, and 5.76 and base values of 0, 0, 2.99, 0, and 0 were given to criteria of X1 to X5, respectively. After determination of ideal and base values, normalized decision matrix was calculated and presented as shown in Eq. (5).

$$C = \begin{matrix} & X1 & X2 & X3 & X4 & X5 \\ A1 & 1.00000 & 0.82606 & 0.00000 & 0.09599 & 0.49306 \\ A2 & 1.00000 & 1.00000 & 0.43285 & 0.77254 & 1.00000 \\ A3 & 1.00000 & 0.94879 & 0.42899 & 0.53433 & 0.31944 \\ \dots & \dots & \dots & \dots & \dots & \dots \\ A50 & 0.00000 & 0.42955 & 0.76618 & 0.90861 & 0.29688 \\ A51 & 0.00000 & 0.23130 & 0.73430 & 0.98223 & 0.18576 \\ A52 & 0.00000 & 0.29738 & 0.80193 & 0.96925 & 0.10938 \end{matrix} \quad (5)$$

3.1.2.2. Determination of preference matrix. After normalization of decision matrix for each K_i , a value matrix was created and was used to determine the value of u (v_{ij}) for each v_{ij} , such that $0 < u(v_{ij}) < 1$. The base preference (priority) criteria, $\pi_{gh}(w_e, w_f)$, between each alternative of w_e and w_f according to each alternative of k_g and k_h were calculated using Eq. (S-9). The result of preference matrix is presented by Eq. (6).

$$P = \begin{matrix} & A1 & A2 & A3 & A50 & A51 & A52 & From above \\ A1 & 0.000 & 0.000 & 0.164 & \dots & 0.464 & 0.498 & 0.493 & 50 \\ A2 & 1.000 & 0.000 & 1.000 & \dots & 0.664 & 0.686 & 0.666 & 2 \\ A3 & 0.836 & 0.000 & 0.000 & \dots & 0.533 & 0.585 & 0.579 & 25 \\ \dots & \dots & \dots & \dots & \dots & \dots & \dots & \dots & \dots \\ A50 & 0.536 & 0.336 & 0.467 & \dots & 0.000 & 0.879 & 0.604 & 38 \\ A51 & 0.502 & 0.314 & 0.415 & \dots & 0.121 & 0.000 & 0.283 & 44 \\ A52 & 0.507 & 0.334 & 0.421 & \dots & 0.396 & 0.717 & 0.000 & 42 \\ From below & 44 & 1 & 21 & \dots & 34 & 46 & 42 & \end{matrix} \quad (6)$$

3.1.2.3. Alternatives ranking in MAPPAC technique. After determination of preference matrix, alternatives were ranked as shown in Table 3.

3.1.3. Calculation stages in ELECTRE technique

3.1.3.1. Normalization. Considering the presence of positive and negative criteria in the decision matrix, the measured values related to negative criteria should be reversed prior to normalization. Therefore, bigger values in decision matrix indicate more desirability of the criteria. Eq. (7) shows the normalized decision matrix (N_D) using Euclidean norm.

$$N_D = \begin{matrix} \begin{matrix} 0.057 & 0.073 & 0.043 & 0.3 & 0.137 \\ 0.057 & 0.035 & 0.109 & 0.079 & 0.124 \\ 0.057 & 0.046 & 0.108 & 0.157 & 0.142 \\ \dots & \dots & \dots & \dots & \dots \\ 0.2 & 0.161 & 0.159 & 0.035 & 0.142 \\ 0.2 & 0.205 & 0.154 & 0.011 & 0.145 \\ 0.2 & 0.19 & 0.164 & 0.015 & 0.147 \end{matrix} \end{matrix} \quad (7)$$

3.1.3.2. Formation of weighted normalized matrix. Eq. (8) shows the weighted normalized matrix obtained by the multiplication of the weighted normalized matrix and diagonal matrix of criteria weights.

$$V = \begin{matrix} \begin{matrix} 0.007 & 0.019 & 0.016 & 0.027 & 0.022 \\ 0.007 & 0.009 & 0.04 & 0.007 & 0.02 \\ 0.007 & 0.012 & 0.04 & 0.014 & 0.023 \\ \dots & \dots & \dots & \dots & \dots \\ 0.024 & 0.042 & 0.059 & 0.003 & 0.023 \\ 0.024 & 0.053 & 0.057 & 0.001 & 0.023 \\ 0.024 & 0.05 & 0.061 & 0.001 & 0.024 \end{matrix} \end{matrix} \quad (8)$$

3.1.3.3. Formation of concordance and discordance matrixes. After determination of concordance and discordance sets, related matrixes were determined using Eqs. (S-5) and (S-6), respectively. Concordance and discordance matrixes are given in Eqs. (9) and (10), respectively.

$$I = \begin{matrix} \begin{matrix} - & 0 & 0.16 & \dots & 0.54 & 0.54 & 0.54 \\ 0.88 & - & 0.88 & \dots & 0.54 & 0.54 & 0.54 \\ 0.72 & 0 & - & \dots & 0.54 & 0.54 & 0.54 \\ \dots & \dots & \dots & \dots & \dots & \dots & \dots \\ 0.46 & 0.46 & 0.46 & \dots & - & 0.79 & 0.42 \\ 0.46 & 0.46 & 0.46 & \dots & 0.09 & - & 0.25 \\ 0.46 & 0.46 & 0.46 & \dots & 0.46 & 0.63 & - \end{matrix} \end{matrix} \quad (9)$$

$$NI = \begin{pmatrix} - & 1 & 1 & \dots & 1 & 1 & 1 \\ 0 & - & 0 & \dots & 0.564 & 0.379 & 0.507 \\ 0.029 & 1 & - & \dots & 0.627 & 0.411 & 0.553 \\ \dots & \dots & \dots & \dots & \dots & \dots & \dots \\ 0.536 & 1 & 1 & \dots & - & 0.189 & 0.261 \\ 0.839 & 1 & 1 & \dots & 1 & - & 1 \\ 0.683 & 1 & 1 & \dots & 1 & 0.1 & - \end{pmatrix} \quad (10)$$

3.1.3.4. Formation of effective concordance and discordance matrixes. In this step, the threshold values of \bar{I} (0.483) and $\bar{N}\bar{I}$ (0.698) were calculated using Eqs. (S-22) and (S-25), respectively. Then, the effective concordance matrix (F) using Eqs. (S-8) and (S-9), and the effective discordance matrix (G) using Eqs. (S-26) and (S-27) were calculated as presented in Eqs. (11) and (12), respectively. The value of 1 in matrix F and also the value of 0 in matrix G indicates that their corresponding element values in matrix \bar{I} and $\bar{N}\bar{I}$ are bigger than the related threshold.

$$F = \begin{pmatrix} - & 0 & 0 & 1 & 1 & 1 \\ 1 & - & 1 & 1 & 1 & 1 \\ 1 & 0 & - & 1 & 1 & 1 \\ \dots & \dots & \dots & \dots & \dots & \dots \\ 0 & 0 & 0 & - & 1 & 0 \\ 0 & 0 & 0 & 0 & - & 0 \\ 0 & 0 & 0 & 0 & 1 & - \end{pmatrix} \quad (11)$$

$$G = \begin{pmatrix} - & 0 & 0 & \dots & 0 & 0 & 0 \\ 1 & - & 1 & \dots & 1 & 1 & 1 \\ 1 & 0 & - & \dots & 1 & 1 & 1 \\ \dots & \dots & \dots & \dots & \dots & \dots & \dots \\ 1 & 0 & 0 & \dots & - & 1 & 1 \\ 0 & 0 & 0 & \dots & 0 & - & 0 \\ 1 & 0 & 0 & \dots & 0 & 1 & - \end{pmatrix} \quad (12)$$

3.1.3.5. Formation of effective general matrix. The effective whole (general) matrix is given in Eq. (13), which is the product of concordance matrix multiplied by discordance matrix.

$$H = \begin{matrix} & \begin{matrix} A1 & A2 & A3 & & A50 & A51 & A52 \end{matrix} \\ \begin{matrix} A1 \\ A2 \\ A3 \\ \dots \\ A50 \\ A51 \\ A52 \end{matrix} & \begin{pmatrix} - & 0 & 0 & \dots & 0 & 0 & 0 \\ 1 & - & 1 & \dots & 1 & 1 & 1 \\ 1 & 0 & - & \dots & 1 & 1 & 1 \\ \dots & \dots & \dots & \dots & \dots & \dots & \dots \\ 0 & 0 & 0 & \dots & - & 1 & 0 \\ 0 & 0 & 0 & \dots & 0 & - & 0 \\ 0 & 0 & 0 & \dots & 0 & 1 & - \end{pmatrix} \end{pmatrix} \quad (13)$$

3.1.3.6. Alternatives ranking in ELECTRE technique. In ELECTRE technique, an alternative is favorable and preference when the column and row of effective general matrix has a maximum value of 0 or 1, respectively. In this study, each alternative score was determined by the summation of elements of each row, and preference alternatives were chosen according to the obtained scores. Table 4 shows the ranking of alternatives.

3.1.4. Final alternatives ranking

All three techniques of ORESTE, MAPPAC, and ELECTRE were used in alternatives ranking to validate the results. The comparative evaluation of the results showed that alternatives 28 and 35 allocated the best ranks among the others using all

Table 4. Alternatives ranking in ELECTRE technique.

Rank	Alt.	Sc.	Rank	Alt.	Sc.	Rank	Alt.	Sc.	Rank	Alt.	Sc.
1	A28	47	13	A20	20	19	A31	10	23	A50	5
2	A35	43		A25	20	20	A4	9	24	A45	3
3	A15	41		A39	20		A23	9		A52	3
4	A2	40	14	A3	17		A29	9	25	A1	2
5	A48	38		A6	17		A30	9		A14	2
6	A12	34		A11	17		A36	9		A27	2
7	A13	33		A37	17		A38	9		A51	2
8	A22	32	15	A49	15		A42	9	26	A34	1
9	A41	31	16	A24	14	21	A33	7	27	A8	0
10	A9	30	17	A17	13	22	A19	6		A21	0
11	A7	28		A26	13		A44	6		A40	0
12	A5	24	18	A16	12	23	A32	5		A43	0
13	A10	20	19	A18	10		A46	5		A47	0

Table 5. Final ranking of alternatives based on averaging from ranking results of all three techniques.

Rank	Min	Alt.	Rank	Min	Alt.	Rank	Min	Alt.	Rank	Min	Alt.
1	1.00	A28	14	13.67	A5	27	22.00	A45	40	31.00	A50
2	2.00	A35	15	14.00	A6	28	24.00	A18	41	31.67	A1
3	2.67	A15	16	14.00	A25	29	24.33	A44	42	32.00	A46
4	3.67	A2	17	14.33	A20	30	24.67	A4	43	34.00	A52
5	5.00	A41	18	15.00	A39	31	25.33	A42	44	34.67	A43
6	6.33	A9	19	16.67	A30	32	26.33	A32	45	35.33	A51
7	7.00	A22	20	18.33	A3	33	26.33	A19	46	35.67	A8
8	7.00	A48	21	19.33	A17	34	27.33	A38	47	36.00	A27
9	7.33	A7	22	19.33	A24	35	27.67	A29	48	36.67	A14
10	7.67	A12	23	19.67	A49	36	28.00	A23	49	38.33	A21
11	8.33	A13	24	20.00	A26	37	29.00	A31	50	38.33	A34
12	11.33	A10	25	20.67	A37	38	29.33	A36	51	38.33	A40
13	12.00	A11	26	21.67	A16	39	30.00	A33	52	39.67	A47

techniques, respectively. The best results in settling experiments were concluded for studied criteria using 5 g/t of A-130 and N-100 flocculants. Regarding the results of ranking difference for other alternatives and also for common ranking between them, the arithmetic average was carried out for ranking results of alternatives ranking (Table 5). As shown in Table 5, the current consuming flocculant in the complex (A-27) at concentrations of 2, 4, 5, and 7 g/t placed in ranks of 9, 17, 39, and 42, respectively.

3.2. Evaluation of pilot settling experiments for non-continuous feeding

Settling flux is calculated using Eq. (14), which is a common criterion to select optimum feed solid content in the thickener. In thickener designing, the feed solid content with the highest settling flux is selected for implementation. The settling flux is calculated from Eq. (14):

$$G_s = U(c) \times C \quad (14)$$

where G_s is settling flux ($t/h/m^2$), $U(c)$ is pulp settling rate (m/h), and C is pulp concentration (t/m^3).

Pilot settling experiments were done using N-100, A-130, and A-27 at a dosage of 5 g/t and settling flux of 2.0, 1.8, and 1.6 ($t/h/m^2$). Figure 3 shows the changes in bed height as a function of time. As shown in Figure 3, while using A-130, N-100, and A-27 flocculants, 3-m height bed was set in 32, 40, and 46 min, respectively. These results are in good agreement with bench scale settling experiments. Based on Eq. (S-29) presented in supplementary file, settling rates obtained in

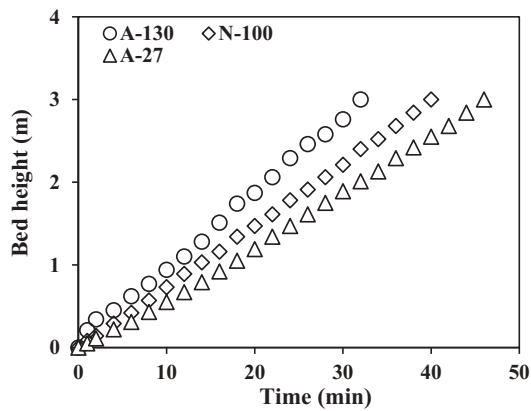


Figure 3. Effect of the chosen flocculants on bed height in non-continuous feeding.

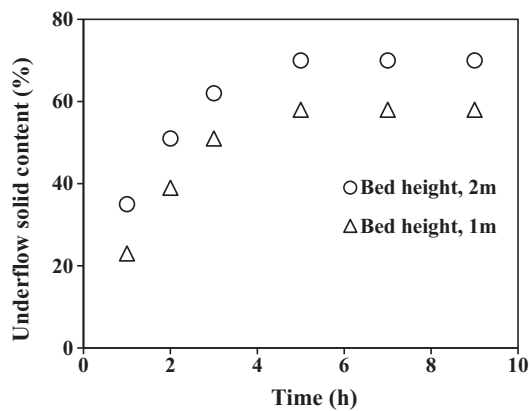


Figure 4. Effect of bed height on underflow solid content in non-continuous feeding (flocculant: A-130).

regard to their flocculant agents are in the following order: A-130 > N-100 > A-27.

Due to higher settling rate of 5 g/t A-130 flocculant, pilot settling experiment was performed at settling flux of 2 t/h/m². In this experiment, a 5 wt.% pulp was introduced at 3 m of height to the thickener and by adjusting bed height at 1 and 2 m, sampling from underflow was performed within 1, 2, 3, 5, 7, and 9 h. Figure 4 shows the effect of bed height on underflow solid content.

The flocs generated from mixing the pulp with flocculant solution in hindered settling zone were gradually contracted through hydrostatic pressure of higher zones as well as the pressure of settling particles layers. As illustrated in Figure 4, the contraction is maximized after 5 h and the most changes of underflow solid content occur in the time range of 1 to 3 h. Besides, by increasing bed height from 1 to 2 m, pressure on layers increases in hindered settling zone. Therefore, underflow solid content clearly increases as a result of water releasing from flocs. In this research, the maximum underflow solid content was achieved at bed height of 1 and 2 m by 58% and 70%, respectively, denoting successful performance of pilot-scale paste thickener in dewatering of Esfordi phosphate tailing.

Table 6. The solid percentage of samples in continuous feeding.

Time (h)	Height (m)					
	0.0	0.5	1.0	1.5	2.0	2.25
0	69.3	60.4	53.8	30.7	7.8	0
1	70.2	64.7	54.0	31.2	9.5	0
2	69.0	61.0	53.6	30.3	10.1	0
3	70.3	63.1	52.9	32.0	9.9	0
4	70.6	62.3	54.5	31.8	11.0	0
5	71.2	62.4	54.3	32.2	10.5	0
Average	70.1	62.3	53.9	31.4	9.8	0
Variance	0.6	2.0	0.3	0.5	1.0	0

3.3. Evaluation of pilot settling experiments in continuous feeding

Under optimum conditions obtained from pilot settling experiments in non-continuous feeding (flocculant of A-130, at a dosage of 5 g/t, bed height of 2 m, time of 5 h, and settling flux of 2 (t/h/m²)), pilot settling experiment was carried out in continuous feeding at 3 m of feeding height for 5 h. Sampling was performed at 1 h intervals from all faucets. The solid percentage in different times and bed heights is given in Table 6.

The results of average solid percentages at different heights (Table 6) indicated that the increase in the solid percentage occurs at 1 to 2 m of height from underflow discharge as a result of the compression process. Within 1 to 2 m of distance from underflow discharge, the increase in the solid percentage rate changes with slower pace due to the declined water content in flocs.

Totally, the basis of particle settling in thickeners is the simple model represented in Figure 5, in which it is divided into three distinct zones including clarification, hindered settling, and compression zones vertically.

The three determined zones can be defined for pilot thickener based on the profile given in Figure 5. The clarification zone is located at 2.25 to 4.0 m of height. The height range between 1.0 and 2.25 m from underflow discharge is allocated to hinder settling. Figure 6 shows the changes in the solid percentage in this zone.

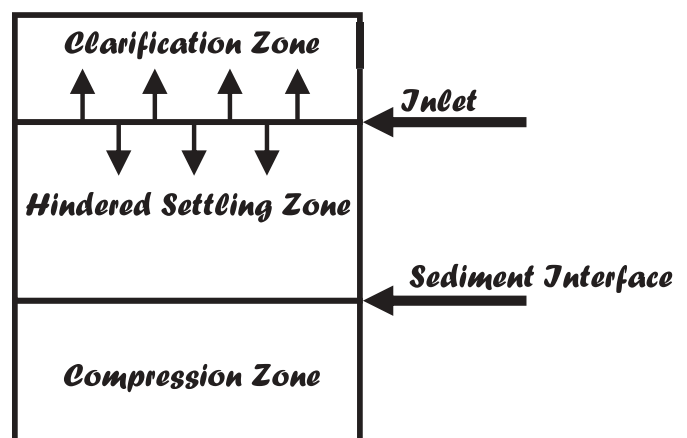


Figure 5. Schematic of the settling zones in a thickener.

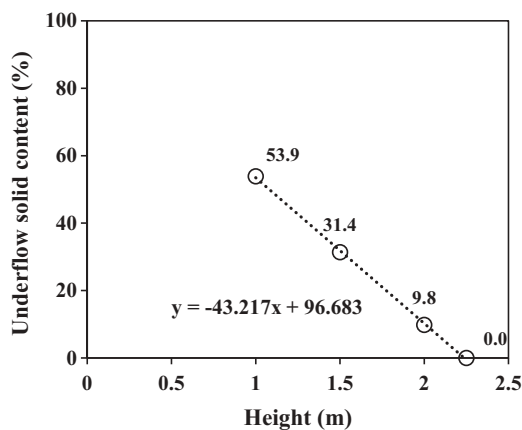


Figure 6. Changes of the solid percentage in the zone of hindered settling (1.0 to 2.25 m).

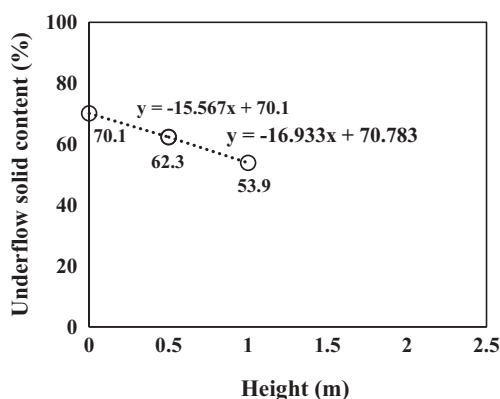


Figure 7. Changes of the solid percentage in the zone of compression settling (0.0 to 1.0 m).

Compression zone (paste formation) is located at 0.0 to 1.0 m of height from the bottom of settling column. The compression zone could be separated into two parts. In the first part, pulp turns into a high concentration slurry (0.5 to 1.0 m). The second part of compression zone is related to the height ranging from 0.0 to 0.5 m from discharge. Figure 7 shows the changes of the solid percentage in this zone. The compression zone is the fundamental difference between conventional and paste thickeners evacuating the maximum water to change the high concentration pulp into a paste.

3.4. Evaluation of yield stress

The paste has a solid-like behavior as concentration is one of its characteristics. Unlike the pulp which principally is liquid and is formed in the shape of its container, paste shape is usually constructed based on its concentration. Pressure is required to flow the paste. This pressure is a rheological terminology recognized as yield stress, which is a unique feature of non-Newtonian fluids.

Within compression process in industrial thickeners, by increasing solid concentration the yield stress increases, consequently paste flow turns into a difficult task. Therefore, regarding the paste thickeners, the increase in the underflow solid content is not the sole criterion for choosing variables

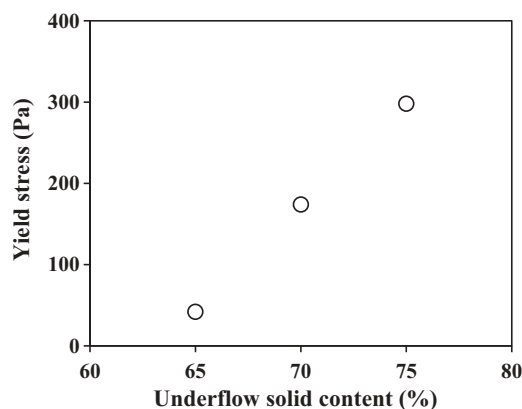


Figure 8. Yield stress as a function of paste solid percentage.

conditions. As discussed earlier, the increase in the solid percentage and yield stress results in a need for higher driving force for rakes leading to the disruption in pump performance to transport paste to the tailings dam.

The slump test is carried out to estimate the yield stress, flow, and competency of paste for disposal. In this research, after measuring the paste slump produced by 5 g/t of A-130 flocculant, yield stress was calculated by Eq. (1). Figure 8 shows the changes in yield stress as a function of paste solid percentage. As shown in Figure 8, yield stress increased significantly. For yield stress, the change is calculated as 250 Pa with the increase in the solid percentage from 65% to 75%.

The results of a study showed that (Wills 2011), the yield stress of 175 to 300 Pa along with a solid percentage of 70–75% is suitable for paste flow and transportation purposes. Hence, design, construction, and implementation of a paste thickener were feasible in the Esfordi phosphate complex.

4. Conclusion

Regarding the feasibility of applying paste thickeners for mineral processing units, in this research a novel procedure was presented for assessment of this equipment in dewatering of phosphate tailings. Firstly, three various MCDM techniques including ORESTE, MAPPAC, and ELECTRE were applied to choose type and concentration of proper flocculants for a paste thickener according to environmental effects of flocculants, flocculant price, particle settling rate, turbidity of overflow water, and underflow water content. The results showed that the first (A-130, 5 g/t) and second (N-100, 5 g/t) ranks are similar for all three techniques indicating validated results. It is highly recommended to use A-130 and N-100 instead of A-27 for further experiments in designing the paste thickener. The results of experiments for measuring bed height in non-continuous feeding state revealed that A-130, N-100, and A-27 flocculants require fewer times to form bed height at 3 m of height from underflow discharge. In case of A-130 flocculant (5 g/t), the results indicated that, 70% of underflow solid percentage was obtained at 2 m of height, at 5 h of residence time, and settling flux of 2 (t/h/m²). Under these conditions for continuous feeding state, clarification,

hindered settling, and compression zones were determined at 2.25–4.0, 1.0–2.25, and 0.0–1.0 m, respectively. Finally, according to the slump test results, the yield stress between 175 and 300 Pa indicates that the paste can flow and be transported by the pumps. The results of the research are promising for solving some environmental effects and lack of water for the Esfordi phosphate plant in case of employing a paste thickener.

Acknowledgments

The authors wish to thank the Iran National Science Foundation (INSF) for providing the facilities to perform this research and financial support.

Disclosure statement

No potential conflict of interest was reported by the authors.

References

- Adibee, N., M. Osanloo, and M. Rahmanpour. 2013. Adverse effects of coal mine waste dumps on the environment and their management. *Environment and Earth Science* 70 (4):1581–92. doi:10.1007/s12665-013-2243-0.
- Alizadeh, S., M. M. Salari Rad, and A. A. Bazzazi. 2016. Alunite processing method selection using the AHP and TOPSIS approaches under fuzzy environment. *International Journal of Mining Science and Technology* 26 (6):1017–23.
- Azimi, R., A. Yazdani-Chamzini, M. M. Fouladgar, E. K. Zavadskas, and M. H. Basiri. 2011. Ranking the strategies of mining sector through ANP and Topsis in a SWOT framework. *Journal of Business Economics and Management* 12 (4):670–89. doi:10.3846/16111699.2011.626552.
- Besra, L., D. K. Sengupta, and S. K. Roy. 1998. Flocculant and surfactant aided dewatering of fine particle suspensions: A review. *Mineral Processing and Extractive Metallurgy Review* 18 (1):67–103. doi:10.1080/08827509808914153.
- Bielecka, M., and J. KrolKorcak. 2010. Hybrid expert system aiding design of post-mining regions restoration. *Ecological Engineering* 36 (10):1232–41. doi:10.1016/j.ecoleng.2010.04.023.
- Boshoff, E. T., J. Morkel, and N. Naude. 2018. Identifying critical parameters in the settling of African kimberlites. *Mineral Processing and Extractive Metallurgy Review* 39 (2):136–44. doi:10.1080/08827508.2017.1391248.
- El-Shall, H., and P. Zhang. 2004. Process for dewatering and utilization of mining wastes. *Minerals Engineering* 17:269–77.
- Garmsiri, M. R., and A. Nosrati. 2019. Dewatering of copper flotation tailings: Effect of feed dilution on the thickener performance. *Mineral Processing and Extractive Metallurgy Review* 40 (2):141–47. doi:10.1080/08827508.2018.1497626.
- Gnandi, K., G. Tchangbedji, K. Killi, G. Baba, and A. I. Ouro Salim. 2005. Processing of phosphate mine tailings by coagulation flocculation to reduce marine pollution in Togo: Laboratory tests. *Mine Water and the Environment* 24:215–21. doi:10.1007/s10230-005-0102-2.
- Gregory, J., and S. Barany. 2011. Adsorption and flocculation by polymers and polymer mixtures. *Advances in Colloid and Interface Science* 169:1–12. doi:10.1016/j.cis.2011.06.004.
- Hayati, M., M. R. Tavakoli Mohammadi, A. Rezaei, and M. R. Shayestehfar. 2014. Risk assessment and ranking of metals using FDAHP and TOPSIS. *Mine Water and the Environment* 33 (2):157–64. doi:10.1007/s10230-014-0263-y.
- Huang, S., X. Li, and Y. Wang. 2012. A new model of geo-environmental impact assessment of mining: A multiple-criteria assessment method integrating Fuzzy-AH with fuzzy synthetic ranking. *Environment and Earth Science* 66 (1):275–84. doi:10.1007/s12665-011-1237-z.
- Kim, S., and A. M. Palomino. 2009. Polyacrilamide-treated kaolin: A fabric study. *Applied Clay Science* 45:270–79. doi:10.1016/j.clay.2009.06.009.
- Kong, R., and M. E. Orazem. 2014. Semi-continuous electrokinetic dewatering of phosphatic clay suspensions. *Electrochimica Acta* 140:438–46. doi:10.1016/j.electacta.2014.07.016.
- Kostovic, M., and Z. Gligoric. 2015. Multi-criteria decision making for collector selection in the flotation of lead–Zinc sulfide ore. *Minerals Engineering* 74:142–49. doi:10.1016/j.mineng.2014.07.019.
- Mahdevari, S., K. Shahriar, and A. Esfahanipour. 2014. Human health and safety risks management in underground coal mines using fuzzy TOPSIS. *Science of the Total Environment* 488–489:85–99. doi:10.1016/j.scitotenv.2014.04.076.
- Mpofu, P., J. Addai-Mensah, and J. Ralston. 2004. Flocculation and dewatering behaviour of smectite dispersions: Effect of polymer structure type. *Minerals Engineering* 17:411–23. doi:10.1016/j.mineng.2003.11.010.
- Mpofu, P., J. A. Mensah, and J. Ralston. 2003. Investigation of the effect of the polymer structure type on flocculation rheology and dewatering behaviour of kaolinite dispersions. *International Journal of Mineral Processing* 71:247–68. doi:10.1016/S0301-7516(03)00062-0.
- Onen, V., P. Beyazyuz, and E. Yel. 2017. Removal of turbidity from travertine processing wastewaters by coagulants, flocculants and natural materials. *Mine Water and the Environment* 1–11. doi:10.1007/s10230-017-0499-4.
- Ozacar, M., and I. Ayhan Sengil. 2003. Enhancing phosphate removal from wastewater by using polyelectrolytes and clay injection. *Journal of Hazardous Materials B100*:131–46. doi:10.1016/S0304-3894(03)00070-0.
- Rahimdel, M. J., and M. Ataei. 2014. Application of analytical hierarchy process to selection of primary crusher. *International Journal of Mining Science and Technology* 24 (4):519–23. doi:10.1016/j.ijmst.2014.05.016.
- Rulyov, N. N., T. A. Dontsova, and V. J. Korolyov. 2005. Ultra-flocculation of diluted fine disperse suspensions. *Mineral Processing and Extractive Metallurgy Review* 26 (3–4):203–17. doi:10.1080/08827500590943965.
- Safari, M., M. Ataei, R. Khalokakaie, and M. Karamozian. 2010. Mineral processing plant location using the analytic hierarchy process – A case study: The Sangan iron ore mine (phase 1). *International Journal of Mining Science and Technology* 20:0691–95.
- Scheiner, B. J., and A. G. Smelley. 1985. The phosphatic clay waste problem —Flocculation as a possible solution. *Mineral Processing and Extractive Metallurgy Review* 1 (3–4):347–61. doi:10.1080/08827508508952597.
- Shen, L., K. Muduli, and A. Barve. 2015. Developing a sustainable development framework in the context of mining industries: AHP approach. *Resources Policy* 46 (Part 1):15–26. doi:10.1016/j.resourpol.2013.10.006.
- Si, H., H. Bi, X. Li, and C. Yang. 2010. Environmental evaluation for sustainable development of coal mining in Qijiang, Western China. *International Journal of Coal Geology* 81 (3):163–68. doi:10.1016/j.coal.2009.11.004.
- Sobczyk, W., A. Kowalska, and E. J. Sobczyk. 2014. The use of ahp multi-criteria method and leopold matrix to assess the impact of gravel and sand pits on the environment of the jasiolka valley. *Mineral Resources Management* 30 (2):157–72.
- Tao, D., B. Parekh, and R. Honaker. 2008. *Development and pilot-scale demonstration of Deep-Cone (TM) paste thickening process for phosphatic clay disposal*. Bartow: Florida Institute of Phosphate Research.
- Wills, B. A., and J. Finch. 2011. *Wills' mineral processing technology: An introduction to the practical aspects of ore treatment and mineral recovery*. 8th ed. Elsevier Science & Technology Books.
- Xu, J. X., H. Zhao, and G. Li. 2014. Geological environmental impact assessment of mining subsidence area based on multilayer fuzzy synthetic evaluation. *Advanced Materials Research* 1010–1012:254–58.
- Zhang, X., L. Gao, D. Barrett, and Y. Chen. 2013. A multi-criteria evaluation of water management for sustainable development in mining. 20th International congress on modelling and simulation, Adelaide, Australia, 482–88.